

# TWO DIMENSIONAL ANALYSIS OF SHALLOW WATER FLOW WITH SUBMERSIBLE LARGE ROUGHNESS ELEMENTS

Tatsuhiko UCHIDA, Graduate student, Department of Civil Engineering, Graduate School of Engineering, Hiroshima University, 1-4-1 Kagamiyama, Higashi-hiroshima 739-8527, Japan, E-mail: utida@hiroshima-u.ac.jp

Shoji FUKUOKA, Professor, Department of Civil Engineering, Graduate School of Engineering, Hiroshima University, Kagamiyama, Higashi-hiroshima 739-8527, Japan, Telephone 081-824-24-7821, fax number 0824-24-7821, E-mail: sfuku@hiroshima-u.ac.jp

## ABSTRACT

In our previous study, we developed a numerical analysis method of flow with non-submersible large roughness elements in group. However, the study on the flow with submersible large roughness elements has not been made enough. The purpose of this paper is to develop a two-dimensional model for shallow water flow with submersible large roughness elements. For this analysis, it is necessary to estimate drag force of roughness elements. Drag forces acting on the submersible elements are measured for various roughness arrangements and water depth. Then, a numerical model is developed through addition of resistance terms due to roughness elements in the two-dimensional shallow water equations using the general curvilinear coordinate system. The applicability of this model is verified by experiments. Additionally, the model is applied to the simulation of flow flooding in an urban district having submersible and non-submersible houses.

Keywords: Submersible large roughness element, drag force, two-dimensional analysis, urban district inundation

## 1. INTRODUCTION

There are many hydraulic problems concerning flows with large roughness, such as foot protection work, bed protective works locating at downstream of weirs, and fishways, and houses in urban inundation areas, and mountainous rivers. In order to design these structures and predict these flows, it is necessary to estimate resistance characteristics of large roughness elements.

Researches has been conducted on the flow resistance resulting from large roughness, using equivalent roughness  $k_s$ <sup>1) 2)</sup>, Chezy coefficient<sup>3)</sup>, Manning roughness coefficient<sup>4)</sup> and friction coefficient  $f$ <sup>5)</sup>. These coefficients are known to vary by arrangements of the roughness elements and flow conditions. In our study<sup>6)</sup>, it was shown that drag force acting on non-submersible large roughness elements could be estimated with enough accuracy under the assumption of hydrostatic pressure distribution using water depth at front and back faces of the element and that two-dimensional shallow water analysis could represent flow with various non-submersible elements.

The purpose of this paper is to develop a two-dimensional model for shallow water flow with submersible large roughness elements. Drag forces acting on submersible large roughness elements and their estimating method are investigated for various arrangements of the roughness elements and different water depth. Thereafter, a numerical model is developed through addition of resistance terms due to submersible roughness elements in the two-dimensional shallow water equations. This model is applied to simulate inundation of an urban district having submersible and non-submersible houses.

## 2. DRAG FORCE OF LARGE ROUGHNESS ELEMENTS

Drag forces acting on large roughness elements were measured in a 10m long and 2.5m wide channel, as shown in Fig.1. The channel bed had 1/500 slope. Drag force measurement instrument was installed inside a pit at 5.7m distance from upstream end of the channel. A 0.2m wide and 0.03m high roughness element, which is rectangular block, was used in the experiment. Fig.2 shows the

layout of the instrument and placement of large an element. The instrument had a movable platform inside the pit. The platform is used to adjust height of the roughness element for accurate force measurement. Drag forces were measured for an arrangement of large roughness elements in rows and columns in the channel to clarify a relationship between drag forces and spacing of the large roughness elements. Hydraulic conditions of the experiment are shown in Table 1. Here,  $L_x$  and  $L_y$  are spacing between roughness elements in the longitudinal and transverse direction respectively.  $B$  is width and  $d$  is height of the roughness elements. Relative depth  $h^*$  is defined by a ratio of water depth  $h$  at 1.0m from upstream end of the channel to the element height  $d$  and is an important parameter for the flow with large roughness elements.

Fig.3 shows longitudinal distributions of drag forces for groups of submersible large roughness elements. Here, relative distance  $X^*$  is a ratio of distance of an element from upstream end of a group elements to total longitudinal length of the group elements. On the other hand, relative force  $F^*$  is defined by  $F^* = F_x/F_0$ . Where,  $F_x$  is a force on an element for its group arrangement and  $F_0$  is a force on the element only for single block in the channel, both having same hydraulic condition. Fig.3 shows even though,  $L_y$  is different in Case1 and Case2 as seen in Table1, drag forces for the inside of the group are almost similar for both the cases. This result indicates that  $L_x$  rather than  $L_y$  affects drag force. Drag forces are extremely smaller for the condition of  $L_x/d=3.3$  compared with other two cases of  $L_x/d$ . Because, the pressure acting on the upstream face of an element is reduced for  $L_x/d=3.3$  due to smaller length of  $L_x$  compared to length of vortex shedding from a just upstream element. As the spacing  $L_x$  increases for  $L_x/d > 3.3$ , velocity approaching to the element recovers toward normal flow condition. Therefore, drag forces for these cases increased with increasing  $L_x$  as shown in Fig.3. The drag force acting on the

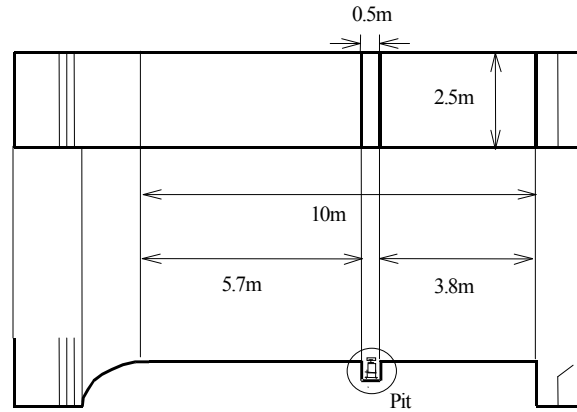


Fig1 Layout of the experimental channel

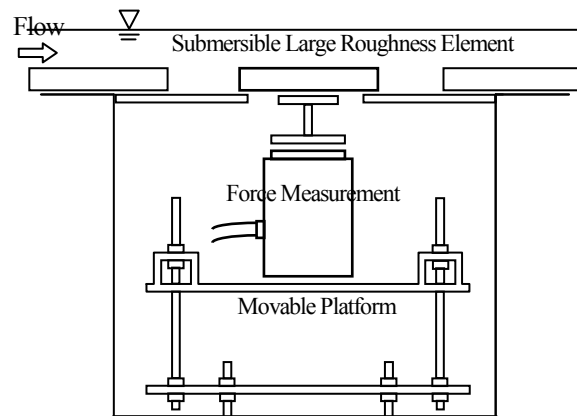


Fig.2 Layout of the drag force measurement instrument

Table1 Hydraulic condition of the measurement

	$L_x/d$	$L_y/d$	Discharge $Q(m^3/s)$	Relative Depth $h^*$
Case1	3.3~20.0	6.7	0.0089~0.00785	1.2~3.1
Case2	3.3~13.3	20.0	0.0089~0.00587	1.0~2.4

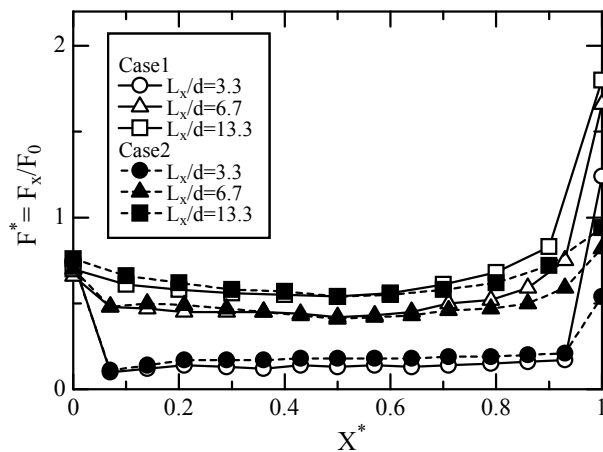


Fig.3 Longitudinal drag force distribution for groups of submersible large roughness elements

roughness elements locating at extreme downstream of a group ( $X^*=1.0$ ) is greater than that of any other roughness elements. This is because of large difference in water depth between front and back of the last roughness elements, which occurs due to difference in resistance inside and outside of the group elements. Therefore, for Case1, in which transverse spacing length  $L_y$  is 3 times shorter compared to Case2, the drag force of the last element is greater than that of Case2. The similar phenomenon occurred in case of non-submersible roughness elements<sup>6)</sup>.

### 3. ESTIMATING METHOD OF DRAG FORCE ACTING ON SUBMERSIBLE LARGE ROUGHNESS ELEMENT

Drag force acting on non-submersible roughness element can be evaluated by equation (1) of hydrostatic distribution<sup>6)</sup>. With the similar assumption of hydrostatic distribution, drag force acting on submersible large roughness element is given by equation (2).

$$F_x = \frac{1}{2} \rho g B (h_1^2 - h_2^2) \quad (1)$$

$$F_x = \rho g B d (h_1 - h_2) \quad (2)$$

Where,  $F_x$ =drag force,  $\rho$  =water density,  $g$ =gravity acceleration,  $h_1$ = water depth at front face of a roughness element,  $h_2$ =water depth at back face of the roughness element.

Fig.4 shows relationships between computed drag forces using actual water depth from equation (1) or (2) and measured drag forces acting on large roughness elements. Triangular symbols indicate non-submersible roughness elements and black round symbols indicate submersible roughness elements of Case2. The black round symbol has different size depending on discharge, and hence relative depth  $h^*$ . A size of the black round symbol increases with the increasing of relative depth  $h^*$ , and the black round symbols having same  $L_x$  are connected by a solid line. For the case of the non-submersible roughness elements, calculated results and measured results are almost similar. For the submersible elements, however, as relative depth  $h^*$  increases, difference between computation and measurement becomes greater. Here, below is an explanation of the above result. As water depth  $h$  increases above the roughness element height, a flow over the elements become established. Under this flow condition, downward component of the flow become large at the downstream area of the submersible roughness element. That means, pressure distribution acting on the back face of the element is smaller than hydrostatic distribution. Therefore, computed result is greater than that of the measurement for submersible roughness element. Above mentioned result

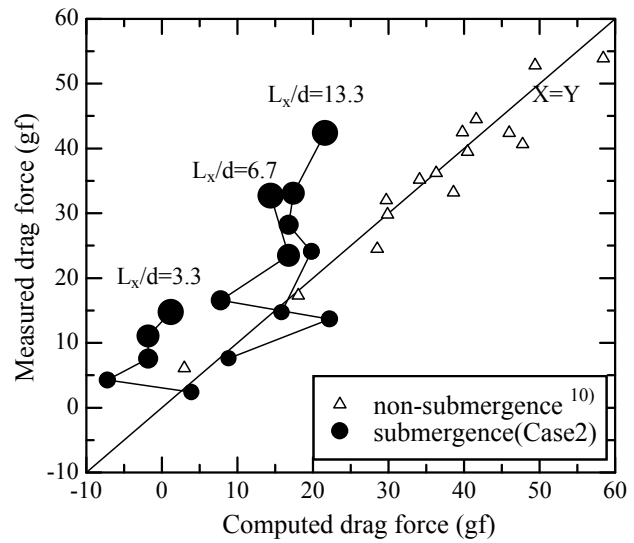


Fig.4 Relationships between computed with an assumption of hydrostatic and measured drag force acting on the submersible large roughness elements

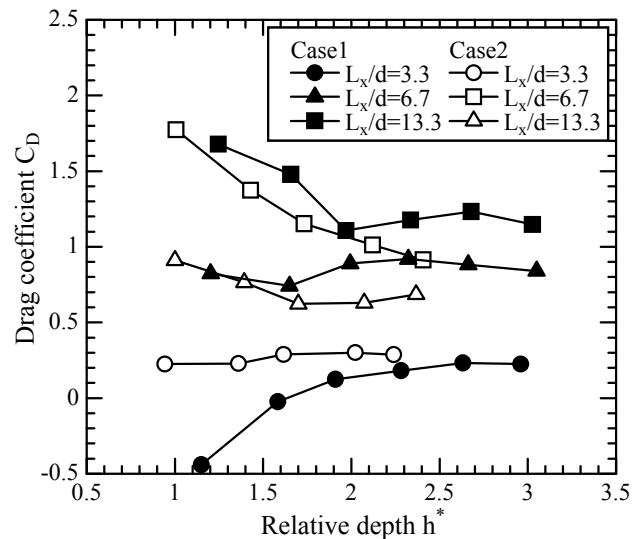


Fig.5 Relationship between drag coefficient and relative depth  $h^*$

Fig.5 Relationship between drag coefficient and relative depth  $h^*$

indicates that drag forces acting on the submersible roughness elements can not be estimated by equation (2).

Therefore, this study investigates drag coefficient  $C_D$  through the equation (3).

$$C_D = \frac{2F_x}{\rho AU^2} \quad (3)$$

Where,  $A$ = a projected area (=dB),  $U$ = a velocity at 1.0m from upstream end of the channel

Fig.5 shows relationships between relative depth  $h^*$  and drag coefficient computed at the center of the submersible roughness groups. Drag coefficient  $C_D$  varies with the elements arrangement and relative depth  $h^*$  as shown in Fig.5. Drag coefficient  $C_D$  is large when relative depth  $h^*$  is small ( $h^* < 2.0$ ). The greater relative depth  $h^*$  becomes, however, the smaller drag coefficients  $C_D$  become, and then, for  $h^* > 2.0$ , drag coefficient  $C_D$  does not change with  $h^*$ . It is considered that, for  $h^* > 2.0$ , the shape and size of vortex motion occurring at a back of roughness elements becomes stable without direct influence by water depth. And variation of drag coefficient  $C_D$  with elements arrangement is relatively small for  $h^* > 2.0$ . So, drag force acting on submersible roughness element can be calculated by equation (3), using a proper drag coefficient  $C_D$  in each roughness arrangement.

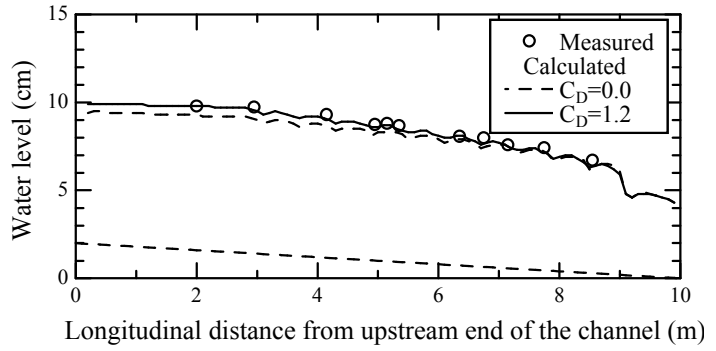


Fig.6 Longitudinal distribution of water depth

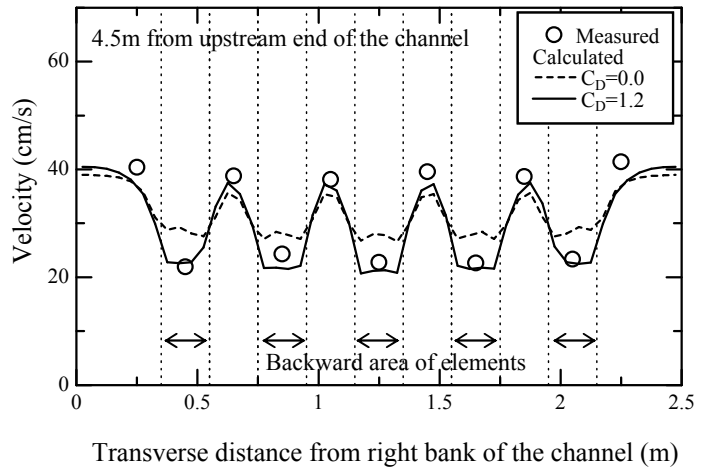


Fig.7 Traverse distribution of streamwise velocity

#### 4. TWO-DIMENSIONAL NUMERICAL ANALYSIS FOR FLOW WITH SUBMERSIBLE LARGE ROUGHNESS ELEMENTS

A two-dimensional shallow water model is developed by employing general curvilinear coordinate system <sup>6)</sup>. The momentum equations include resistance terms for submersible large roughness elements. The resistance terms, which mean  $F_x$  in equation (3), are given at immediate upstream meshes of the submersible elements. Bed level of computation meshes at roughness element is raised by the element height (and hence  $d$ ). For the computation, experimental discharge at upstream end and critical depth at downstream end were given as boundary condition. The slip-condition is applied for both the sidewall of the channel. The calculation continues routinely by using forward difference of time until discharge becomes stable, and gets the final output of the computation.

The following are comparisons between computed and experimental result for  $L_x/d=13.3$  of Case1. Fig.6 shows a longitudinal distribution of water depth. The water level computed without resistance terms is lower than measured water level due to underestimation of resistance of the elements. The water level computed with resistance terms, however, is almost similar to that of the experiment. Fig.7 shows comparison of transverse distribution of streamwise velocity between computed and measured result. Computed velocity without resistance terms is not reduced for backward area of the elements compared with that of the experiment. With resistance terms, however, computed velocity is almost similar to that of the experiment. The above results indicate that the model, which involves the resistance terms with a proper drag coefficient  $C_D$ , is appropriate for a numerical analysis of flow with submersible large roughness elements.

## 5. APPLICATION OF THE MODEL FOR AN URBAN INNUNDATION WITH NON-SUBMERSIBLE AND SUBMERSIBLE HOUSES

In our previous study, horizontal two-dimensional model accurately simulated the inundation of an urban district with non-submersible houses. However, houses near probable failure locations of a levee and low ground level area are in risk of flooding. The urban houses may have both submersed and non-submersed. Therefore, a numerical model is required to predict an inundation not only for non-submersible houses but also for submersible houses. In this chapter, an inundation in an urban district is assumed, for a location where comparatively large number of submersible houses exist. The model, which was discussed in the proceeding chapter, is applied for a randomly arrangement of submersible and no-submersible large roughness elements.

Fig.8 shows computational mesh with arrangement of the elements. A main street is assumed in the center of the urban district as shown in Fig.8. All flow velocities entering into the mesh over the non-submersible element are given zero as boundary condition. And the resistance terms for the non-submersible element are calculated by using equation (1). For submersible element, bed level of meshes under the element is raised by the element height, and the resistance terms are calculated by equation (4). For the flow with the submersible and non-submersible elements, it is not appropriate to use velocity at upstream of the group elements for equation (4) as discussed in the proceeding chapter. Instead of that, the velocity at a point, where the resistance terms are given, is used in equation (4).

$$F_x = -\frac{1}{2} C_D u_x \sqrt{u_x^2 + u_y^2} \frac{db' \sin \theta}{A'} \quad (4)$$

$$F_y = -\frac{1}{2} C_D u_y \sqrt{u_x^2 + u_y^2} \frac{db' \sin \theta}{A'}$$

Where,  $F_x$  and  $F_y$ =drag force of x and y direction,  $u_x$  and  $u_y$ =velocity of x and y direction,  $b'$ = element width in a grid,  $A'$ = area of a grid,  $\theta$ = angle between U and front face of the element ( $0 \leq \theta \leq \pi$ )

Fig.9 shows longitudinal water level profiles for computation and measurement. The computed result differs a little from the measured result near 7.5m from upstream end of the channel. Distortion of the mesh and the misplacement of the element due to sidewall of the channel are considered as the reason for that difference. But as a

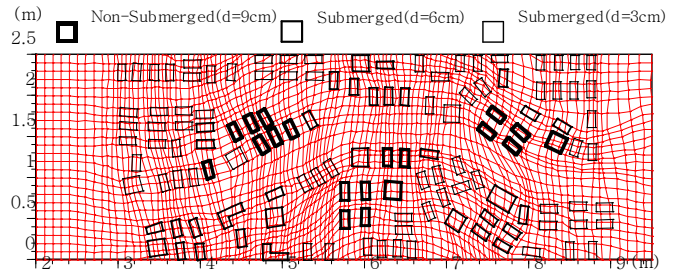


Fig.8 Computation mesh with the elements arrangement

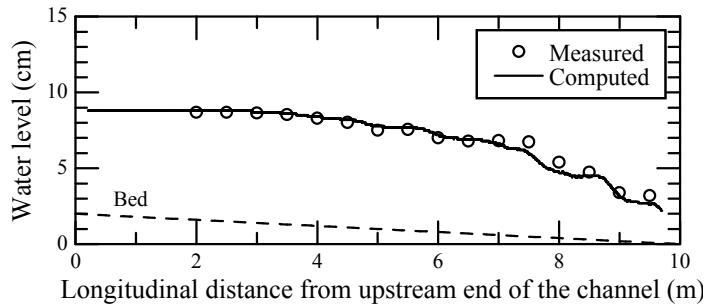


Fig.9 Longitudinal water level profile by computation and measurement

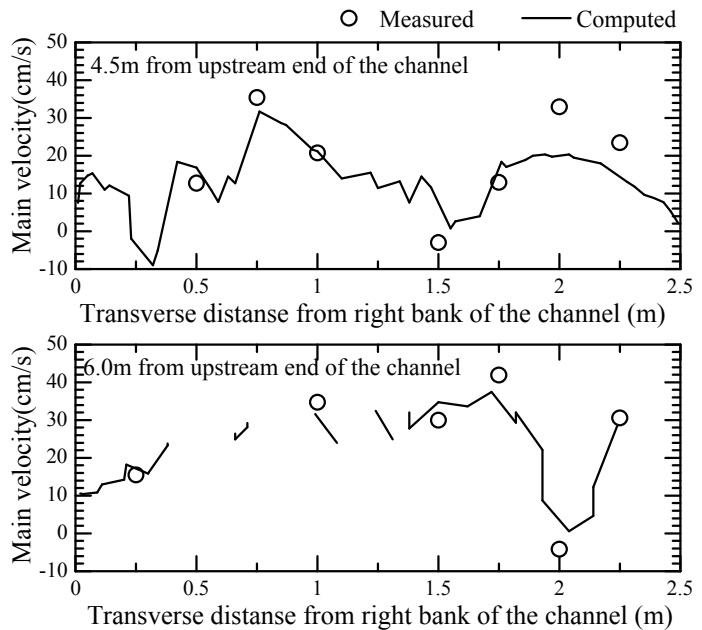


Fig.10 Comparison between computed and measured results for transverse distribution of streamwise velocity

whole, computed water depth is almost similar to measured water depth. Since an actual urban district does not have the boundary channel sidewall, these errors can not occur. It can be considered, therefore, that the numerical model can evaluate resistance of the elements with high accuracy. Fig.10 and Fig.11 show the comparison between computed and measured results of transverse distribution of velocity and velocity vector respectively. Concentrating high flow occurs in the main street. The measured results are almost reproduced by the computation.

The above indicates that the numerical model is applicable to simulate the inundation in urban district with randomly located submersible and non-submersible houses.

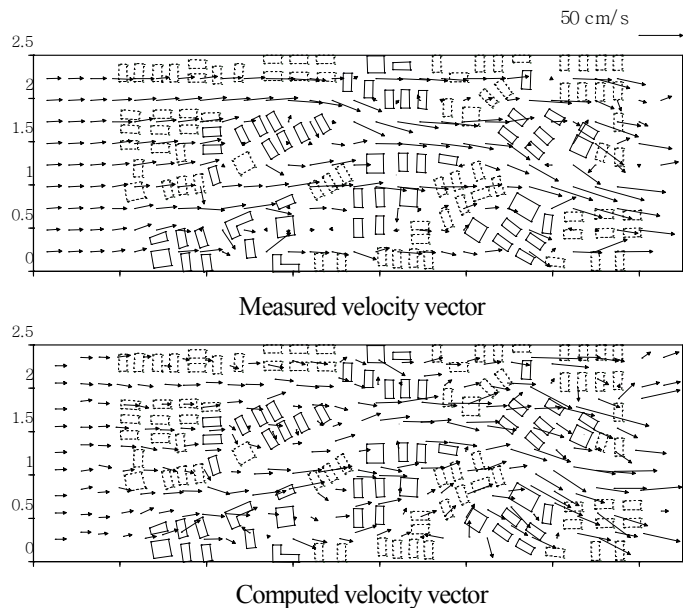


Fig.11 Comparison between measured and computed velocity vector

## 6. CONCLUSION

1. Drag force acting on a submersible large roughness element inside of a group of the element is effected by longitudinal spacing  $L_x$  rather than transverse spacing  $L_y$ . The drag force of the element locating at extreme downstream of the group elements is greater than that of any other elements.
2. Drag force acting on submersible large roughness element cannot be estimated by an assumption of hydrostatic pressure distribution due to establishment of flow over the element. Instead of that, the drag force can be estimated by using a proper drag coefficient  $C_D$  in each roughness arrangement.
3. The two-dimensional model describes the flow accurately with the submersible elements because of proper estimation of resistance of the elements. It also shows that the model is applicable to simulate the inundation in an urban district with randomly located submersible and non-submersible houses.

## REFERENCE

1. Shohei ADACHI: EXPERIMENTAL STUDY ON ARTIFICIAL ROUGHNESS, Proc. of Japan Society of Civil Engineer NO.104, pp. 33-44, 1964
2. Shoji FUKUOKA, Koichi FUJITA and Katsushi MORITA: Hydraulic roles of revetment, Civil Engineering Journal vol.30, pp115-120, 1988
3. Sayre, J.B. and Albertson, M.L.: Roughness spacing in rigid open channels, Proc. of ASCE, Vol.87, HY3, pp.121-150, 1961
4. Herbich, J.B. and Shulits, S.: Large-scale roughness in open-channel flow, Proc. of ASCE, Vol.90, HY6, pp.203-230, 1964
5. Tohru KANDA and Katsushi SUZUKI: Characteristics of resistance to shallow water flows over bed roughened with spheres, Journal of Hydraulic, Coastal and Environmental Engineering No.357, pp.65-74, 1985
6. Shoji FUKUOKA, Mikio KAWASHIMA, Hiroshi YOKOYAMA and Masanori MIZUGUCHI: The numerical simulation model of flood-induced flows in urban residential area and the study of damage reduction, Journal of Hydraulic, Coastal and Environmental Engineering No.600, pp.23-36, 1998